

Mid InfraRed Instrument (MIRI) Cooler Cold Head Assembly Acceptance Testing and Characterization

M. Petach, M. Michaelian

Northrop Grumman Aerospace Systems
Redondo Beach, CA 90278 USA

ABSTRACT

The Cooler Subsystem for the Mid InfraRed Instrument (MIRI) of the James Webb Space Telescope (JWST) utilizes a remotely mounted Cold Head Assembly as the final cooling stage of the pre-cooled Joule-Thomson cooler. The cooler's Cold Head Assembly recently completed its acceptance testing. This paper describes the Cold Head Assembly and summarizes the cryogenic refrigeration performance results. These results are compared with theory and program requirements. These results are also compared to the test results from the flight-like model which preceded it, which was used in the JWST ISIM Cryo-Vac#1 testing.

INTRODUCTION

The Mid InfraRed Instrument Cooler Subsystem (MIRI Cooler) is a closed-cycle helium Joule-Thomson (JT) cryocooler pre-cooled by a three-stage pulse tube cryocooler. The basic architecture and design parameters of this cooler have been described previously [1,2,3,4,5]. The MIRI Cooler consists of four major subassemblies which are integrated into the spacecraft separately and then interconnected. These four subassemblies (Figure 1) are:

- The Cryocooler Electronics Assembly (CEEA)
- The Cryocooler Compressor Assembly (CCA)
- The Cryocooler Tower Assembly (CTA)
- The Cold Head Assembly (CHA)

This paper focuses on the Cold Head Assembly (CHA), which is the remote JT 'cold head' that resides within the JWST observatory's Integrated Science Instrument Module (ISIM). The CHA consists of the JT restriction (which provides the pressure drop for JT cooling), the remote recuperator (which provide the thermal isolation between the 6 K and the 18 K gas), the Optical Module heat exchanger (OMHX) (which conducts heat from the instrument into the cold helium gas), as well as bypass valves (which reroute helium flow for bypass operation as opposed to JT cooling operation).

The cryocooler's Flight Model Cold Head Assembly (FM CHA) is shown in Figure 2 and has recently completed its acceptance testing, including refrigeration performance testing.

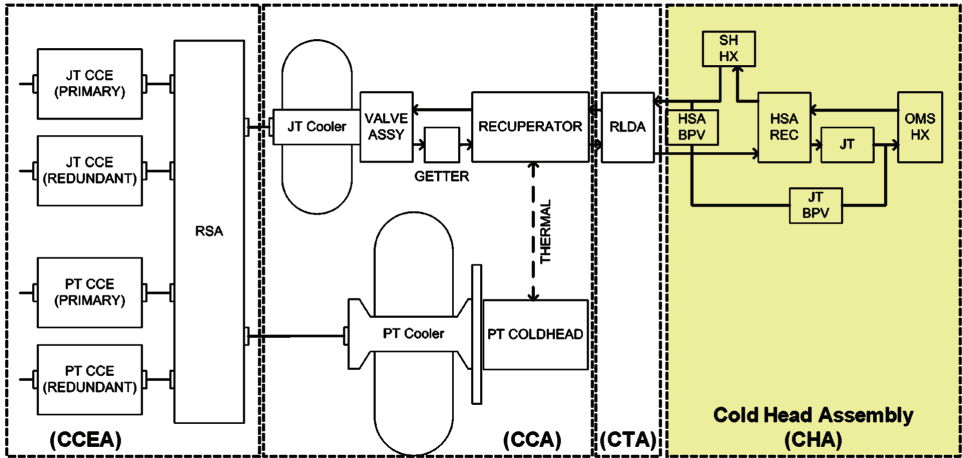


Figure 1. Block diagram indicating the key flight components under test. The MIRI Cooler Subsystem Block Diagram from reference [5] has the flight components. “SH HX” indicated the OM shield heat exchanger. “JT” stands for Joule-Thomson, “CCE” stands for Cryocooler Control Electronics, “RSA” stands for Relay Switch Assembly, “RLDA” stands for Refrigerant Line Deployment Assembly, and “BPV” stands for Bypass Valve. “HSA REC” is the lowest temperature recuperator, and “OMS HX” is the low temperature heat exchanger which removes the load from the MIRI optical bench and its focal plane modules.

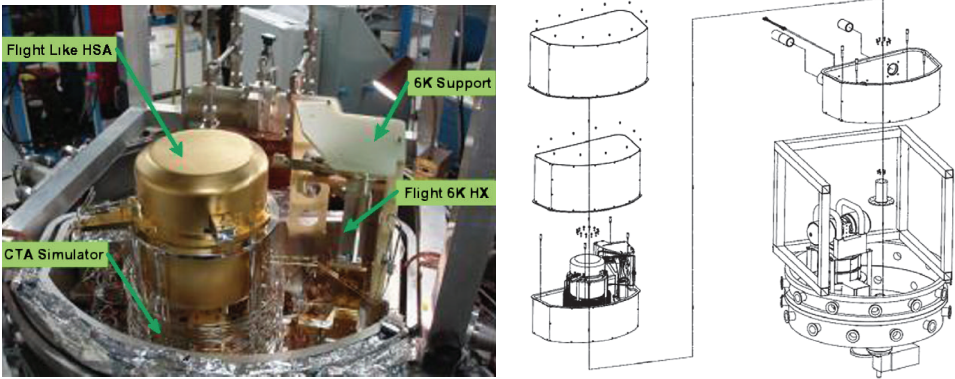


Figure 2. Acceptance test configuration used to verify the refrigeration performance of the flight Cold Head Assembly.

COOLER SUBSYSTEM PERFORMANCE TESTING

Refrigeration performance testing of the FM CHA was performed in a fashion similar to that used to demonstrate the Development Model (DM) Cooler, as described in Reference 5. Performance testing was conducted in a complete “end-to-end” cooler configuration, with Development Model components used in place of flight components everywhere except the Flight Model Coldhead Assembly. The DM Pulse Tube precooler, the DM precooler recuperator, the helium tubing representing the length of the CTA tubing, and the Flight Model remote Cold Head Assembly were all tested within the 36 inch bell-jar vacuum chamber shown in Figure 2. This chamber included cooled shields to simulate the ~40 K cold environment inside the Integrated Science Instrument Module (ISIM) of the JWST Observatory. The rejected heat was removed from the compressor flight interfaces using conventional laboratory recirculating chillers.

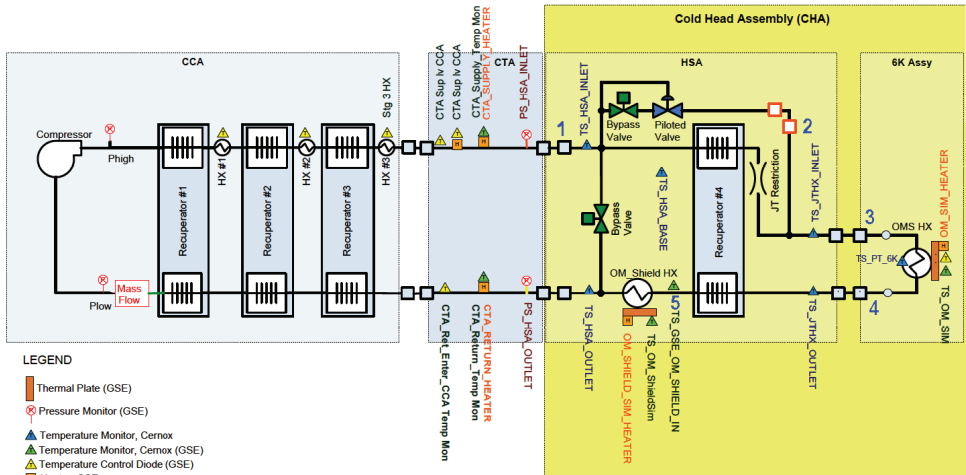


Figure 3. Instrumentation of temperature, pressure, mass flow, and applied load at various location along the JT cooler flow path. Triangles indicated temperature measurement, squares indicate heaters, circles indicate pressure measurements; the larger rectangle indicates a mass flow measurement location. These measured parameters are used to check cooler performance against predictions, and to define subassembly interface requirements.

The test facility and the hardware under test were extensively instrumented as noted in Figure 3. This figure details the instrumentation layout along the JT helium flow circuit that allowed subassembly performance, as well as overall refrigeration performance to be assessed. The electrical power required by the compressors was measured with laboratory digital power meters. Resistive heaters were used to apply the explicit heat loads and simulate the parasitic loads that are required for the flight operation of the instrument. Laboratory grade voltage and current measurements of these heaters were used to determine heat loads. Temperatures at various locations along the JT flow circuit were monitored using CernoxTM temperature sensors. The helium mass flow was measured with conventional laboratory equipment. The helium pressures were measured at the JT compressor ports and the supply and return ports of the CHA using conventional laboratory pressure gauges.

Cooling lift at the OM heat exchanger was measured as a function of temperature, both in the initial cool-down, or “bypass” mode where the precooled helium gas bypasses the Joule-Thomson restriction and passes directly through the OM heat exchanger, and in the Joule-Thomson mode. The equivalent of 475 W of bus power is supplied to the cooler during the cooldown, and the equivalent of 400 W is supplied when data are taken around the steady state temperature. The thermal rejection temperature of the pre-cooler compressors is controlled with an actively controlled liquid cooled heat exchanger. The required 18 K refrigerant line heat loads are applied to the resistive heaters in close thermal contact with the refrigerant lines and the HSA structure. The electrical power applied to the OM HX is then adjusted to achieve the desired OM HX temperature. From these data, the maximum OM heat exchanger load at full bus power, both at the pinch point and at steady state, were measured.

RESULTS AND ANALYSIS

The measured refrigeration lift at the OM HX as a function of the OM HX temperature is shown in Figure 4. In addition to the refrigeration at the OM HX, the cooler also simultaneously lifts “18K” line loads equivalent to the sum of the flight required loads from the ISIM’s actively cooled shield and from the parasitic load on the refrigeration line as they traverse the spacecraft. The power to the compressors is equivalent to the allocated power allowed by the flight requirements, and the reject temperature at the compressor interfaces is the maximum as defined by the

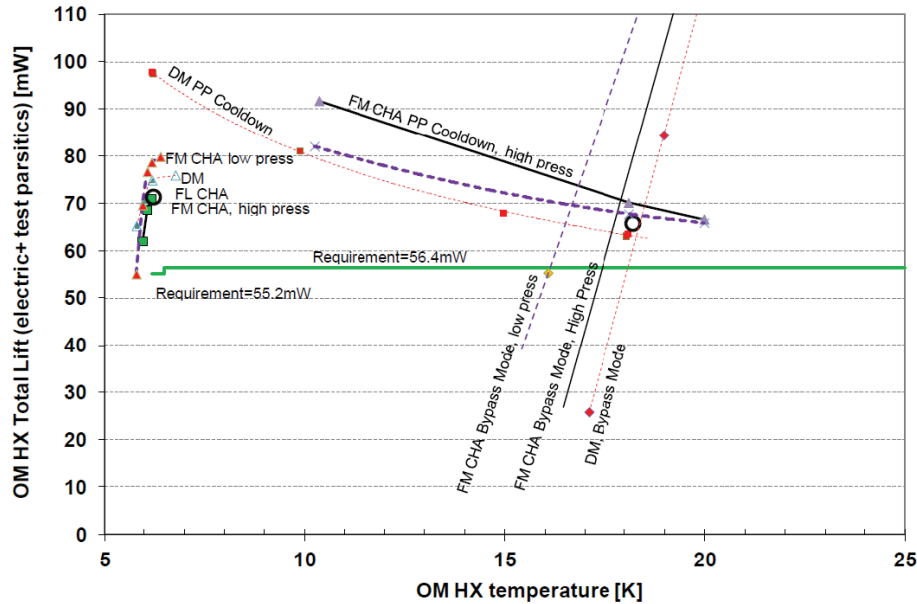


Figure 4. Measured refrigeration performance data points, compared to the program requirements. Data from three different hardware sets are plotted: a) FM HSA and FS 6K HX tested in ATP1a b) FL HSA and FM 6K HX tested in ATP1c, and c) DM HSA and DM 6K HX Cooler in the DM Test. Data for refrigeration lift vs. temperature for the three operating modes of the cooler (bypass mode cool down, pinch point traverse, and steady state operation) are shown.

Table 1. Bus power, reject temperature and 3rd stage loads applied during the measurement of cooler’s refrigeration performance at the OM HX

	Bus Power Allocation	Reject temperature	3 rd stage heat load on the “18K lines”
Cooldown	475 Watts DC	315K	203 mW
Steady State	400 Watts DC	315K	232 mW

flight requirements. The conditions corresponding to the operating modes in Figure 4 are summarized in Table 1.

The measured data for the FM CHA are plotted in Figure 4 along side the data from the DM CHA [5] and the data from the “flight like” CHA configuration. The “flight like” CHA has flight pedigree components everywhere except in the bypass valve, which is a non-flight early generation valve, and the decontamination valve, which is not present. The three CHA configurations for the three hardware instances tested and plotted in Figure 4 are summarized in Table 2.

The lift vs. temperature characteristic of the cooler spans three operating modes. The first of these is the initial cool down, which is done in by circulating cold helium from the precooler while bypassing the remote recuperator and the JT restriction. In this “bypass mode cool down” mode the

Table 2 The three CHA hardware instances and their configurations as tested.

Test configuration	CCEA	CCA	CTA	CHA Refrigerant lines	CHA HSA	CHA OM HX
“DM”	Lab Elec	DM	Simulated	Simulated	DM	
“ATP1c”	Lab Elec	DM	Simulated	Simulated	FL	FM
“ATP1a”	Lab Elec	DM	Simulated	Simulated	FM	FS

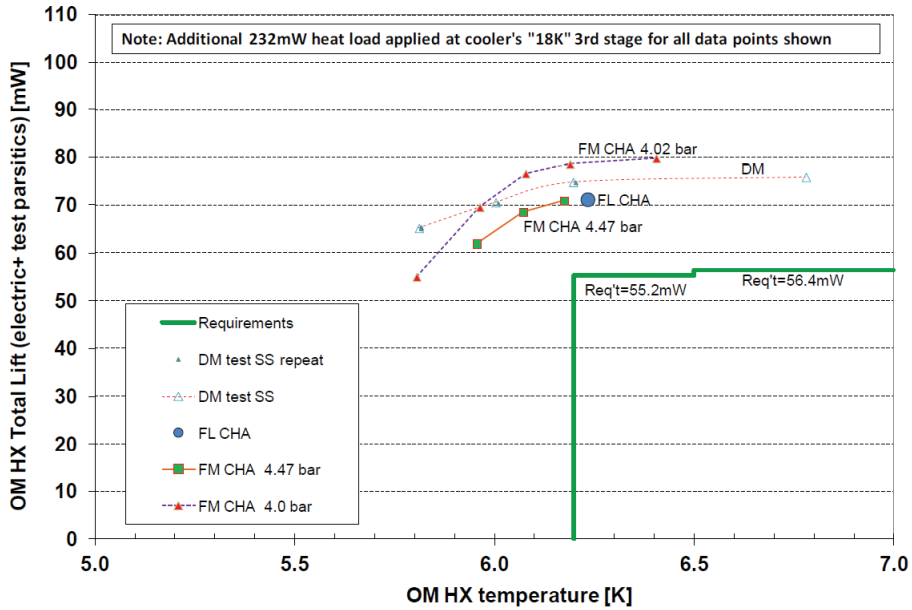


Figure 5. Expanded view of the measured cooler performance in the steady state (science acquisition) temperature region as measured on three instances of the CHA hardware. Again, data from the following are plotted: a) FM HSA and FS 6K HX tested in ATP1a is shown for two different helium fill pressures. The solid triangle data points are the measured data points for a return pressure of approx 4.02 bar, with a dashed line connecting these points simply to guide the eye. The square points are the measured data points for a return pressure of approx 4.57 bar, with a solid line connecting these points simply to guide the eye. b) FL HSA and FM 6K HX tested in ATP1c: The large circular point is the measured data point for this test. c) DM HSA and DM 6K HX Cooler in the DM Test: The unfilled small triangle points are the measured data points for this test with a dashed line connecting these points simply to guide the eye.

OM HX lift vs. temperature has the characteristic linear decrease in lift with temperature of the Pulse tube precooler. When the temperature is well below the JT inversion temperature of approximately 30 K (typically at approximately 16 K-18 K), the helium is sent through the JT recuperator and restriction. The additional refrigeration provided via the Joule-Thomson effect causes the refrigeration to increase as the temperature drops. Once the OM HX has reached the requisite 6.2 K the cooler switches to the third, “steady state” mode. In steady state mode the cooler’s input power is reduced to meet the steady state science power allocation, which reduces the refrigeration lift.

The required minimum lift at the OM HX is shown in Figure 4 as the horizontal line. The lift in all hardware instances and in all cooler modes is seen to meet the requirement.

The data in the steady state science mode is shown again in Figure 5, with the scales expanded so that the data points corresponding to the three different hardware instances can be identified. In this figure, as in Figure 4, the lines connecting the data points are purely to guide the eye.

The measured data in steady state can be compared with a simple lumped thermodynamic model in order to determine how effective the CHA is compared to an ideal system. The simple lumped model consists of a lumped recuperator with an effectiveness of ϵ followed by an isenthalpic restriction and an ideal heat exchanger. The recuperator effectiveness [Reference 6], is defined as the ratio of the actual enthalpy exchange between the high and low pressure gas streams to the maximum possible enthalpy exchange between them, $\epsilon = \delta H_{\text{actual}} / \delta H_{\text{max}}$. Note that which one of the two streams has the limiting heat capacity changes depending upon the pressures of operation, so the limiting δH_{max} must be ascertained for each operating point. The enthalpies at the state points labeled “1” and “5” in Figure 3 are determined from the known temperatures and pressures and the NIST published values for helium enthalpy as a function of temperature and pressure [7,8]. The ideal refrigeration based on the CHA’s incoming helium gas temperature and pressure, and its

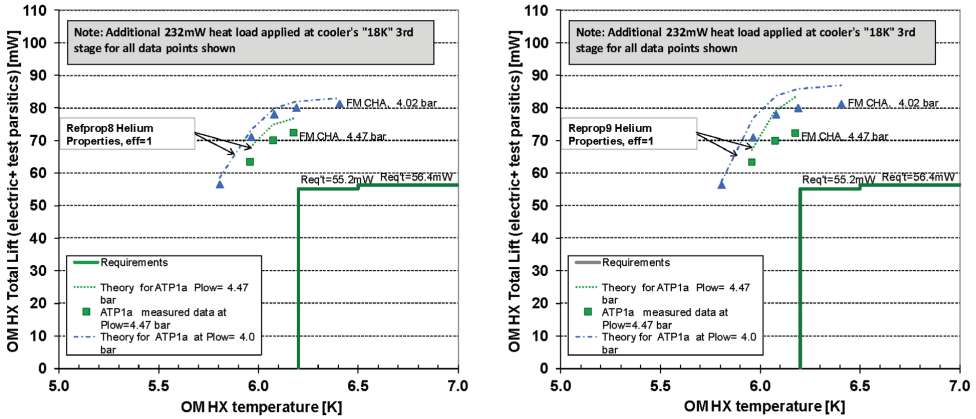


Figure 6. Comparison of measured refrigeration to theory using helium Properties from NIST Refprop 8. Recuperator effectiveness of 99.85% provides best match of theory to data.

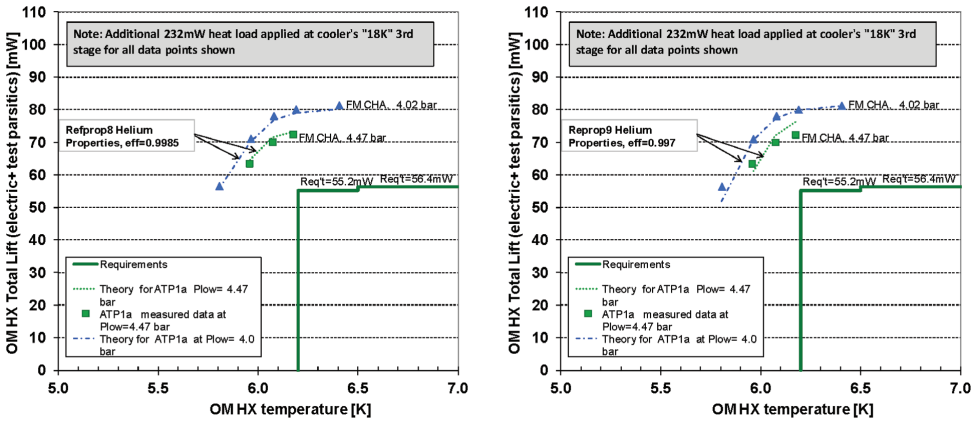


Figure 7. Comparison of measured refrigeration to ideal lumped theory using helium properties from NIST Refprop 8 and Refprop 9.

return gas pressure can then be determined using an effectiveness of $\epsilon = 1$, which is compared to the measured data for steady state operation at two different fill pressures (Figure 6). Since there was a significant change in the published helium properties in the region of temperature and pressure that the CHA operates that occurred [7,8] during the time frame of these tests, both Figures 6 and 7 show comparisons against both versions of the published helium properties. The actual effectiveness (which in this case includes not only the effectiveness of the recuperator but all the potential heat transport through the bypass circuit) is that which results in the lumped model best matching the data. As shown in Figure 7, this "best match" effectiveness ranges from $\epsilon = 99.70\%$ to $\epsilon = 99.85\%$, depending on whether NIST properties from 2007 [7] or 2013 [8] are used. This indicates that the combined recuperator and valve effectiveness is very near the ideal limit.

CONCLUSION

The measurements reported here demonstrate the ability of the MIRI Cooler's Coldhead Assembly to meet the MIRI cooling requirements within the allocated power and thermal rejection constraints. The end-to-end cooler performance as a function of helium fill pressure was characterized, providing a basis for determining the optimal fill pressure for the flight cooler. The comparison between the DM, the FL-HSA, and the FM HSA Cold Head Assemblies shows that the design and manufacturing techniques are well understood and captured. The comparison of the measured

refrigeration performance to a simple four-port thermodynamic model indicates that the refrigeration performance is near ideal and is well understood.

ACKNOWLEDGMENT

This work was funded by NASA and managed by the Jet Propulsion Laboratory, California Institute of Technology.

REFERENCES

1. D. Durand, J. Raab, R. Colbert, M. Michaelian, T. Nguyen, M. Petach, and E. Tward, "NGST Advanced Cryocooler Technology Development Program (ACTDP) Cooler System," *Advances in Cryogenic Engineering*, vol. 51, edited by J. G. Weisend II (2006), pp. 615-622.
2. D. Durand, R. Colbert, C. Jaco M. Michaelian, T. Nguyen, M. Petach, and E. Tward, "NGST Advanced Cryocooler Technology Development Program (ACTDP) Cooler System," *Cryocoolers 14*, ICC Press, Boulder, Colorado (2007), pp. 21-29.
3. D. Durand, R. Colbert, C. Jaco M. Michaelian, T. Nguyen, M. Petach, and J. Raab, "Mid InfraRed Instrument (MIRI) Cooler Subsystem Prototype Demonstration," *Advances in Cryogenic Engineering: Transactions of the Cryogenic Engineering Conference – CEC*, vol. 53, edited by J. G. Weisend II (2008), pp. 807-814.
4. D. Durand, D. Adachi, D. Harvey C. Jaco, M. Michaelian, T. Nguyen, M. Petach, and J. Raab, "Mid InfraRed Instrument (MIRI) Cooler Subsystem Design," *Cryocoolers 15*, ICC Press, Boulder, Colorado (2009), pp. 7-12.
5. M. Petach, D. Durand, M. Michaelian, J. Raab, and E. Tward, "MIRI Cooler System Design Update," *Cryocoolers 16*, ICC Press, Boulder, Colorado (2011), pp. 9-12.
6. B. Maytal, J. M. Pfothhauer, "Miniature Joule-Thomson Cryocooling Principles and Practice," *International Cryogenics Monograph Series*, Springer, New York (2013).
7. E.W. Lemmon, M.O. McLinden, M.L. Huber, "NIST standard reference database 23: REFPROP: Reference fluid thermodynamic and transport properties, (8.0)," National Institute of Standards and Technology, Standard Reference Data Program, Gaithersburg, 2007.
8. E.W. Lemmon, M.L. Huber, M.O. McLinden, "NIST Standard Reference Database 23: Reference Fluid Thermodynamic and Transport Properties-REFPROP, Version 9.1," National Institute of Standards and Technology, Standard Reference Data Program, Gaithersburg, 2013.